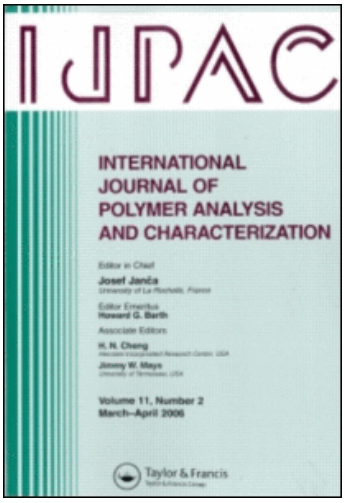

International Journal of Polymer Analysis and Characterization
Publication details, including instructions for authors and subscription information:
http://www.informaworld.com/smpp/title~content=t713646643

Microphase Separation in a Model Graft Copolymer

W. D. Dozier[ab]; D. G. Peiffer[bc]; M. Y. Lin[bd]; M. Rabeony[bc]; P. Thiyagarajan[ab]; S. K. Behal[bc]; M. M. Disko[bc]
[a] Intense Pulsed Neutron Source, Argonne National Laboratory, Argonne, IL [b] Dept. of Physics, Illinois Wesleyan University, Bloomington, IL [c] Exxon Research & Engineering Co., Annandale, NJ [d] Reactor Radiation Division, Gaithersburg, MD

To cite this Article Dozier, W. D. , Peiffer, D. G. , Lin, M. Y. , Rabeony, M. , Thiyagarajan, P. , Behal, S. K. and Disko, M. M.(1995) 'Microphase Separation in a Model Graft Copolymer', International Journal of Polymer Analysis and Characterization, 1: 3, 259 — 275
To link to this Article: DOI: 10.1080/10236669508233879
URL: http://dx.doi.org/10.1080/10236669508233879

Int. J. Polymer Analysis & Characterization
1995, Vol. 1, pp. 259–275
Reprints available directly from the publisher
Photocopying permitted by license only

Microphase Separation in a Model Graft Copolymer

W. D. DOZIER,[a] D. G. PEIFFER,[b] M. Y. LIN,[c] M. RABEONY,[b] P. THIYAGARAJAN,[a] S.K. BEHAL[b] and M. M. DISKO[b]

[a]*Intense Pulsed Neutron Source, Argonne National Laboratory, Argonne, IL 60439*
[b]*Exxon Research & Engineering Co., Rt. 22 East, Clinton Township, Annandale, NJ 08801*
[c]*Reactor Radiation Division, NIST Route 117 and Quince Orchard Rd., Gaithersburg, MD 20899*

We present a preliminary overview of our work on a series of graft copolymers having poly(ethyl acrylate) backbones with pendant chains of polystyrene. The copolymer system appeared to be strongly segregated and exhibited evidence of ordered structures. We observed a lamellar structure in a material containing 20 wt% of polystyrene. Samples under uniaxial strain showed either conventional (i.e., affine deformation) and anomalous ("butterfly" isointensity patterns) behavior in small-angle neutron scattering.

INTRODUCTION

Because the entropy of mixing of polymers is typically very small, any repulsive interaction will result in blends that are, over some temperature range, unstable with respect to phase separation [1]. Therefore, the production of useful polymer blends typically requires the use of compatibilizers, which enhance mixing by limiting the size of domains that result from the phase separation of incompatible homopolymers. It is well established that compatibilizers enhance blend properties [2]. These materials are usually graft or block copolymers in which chain segments interact and "bridge" the interfacial boundary of the phase separated regions. Compatibilization is often effected by the formation of graft copolymers *in situ* under reactive processing conditions [3,4].

The understanding of the phase behavior of diblock copolymers has progressed considerably in recent years [1]. Whereas diblocks are important both in their own right and as tractable model materials, the study of other, more complex copolymer architectures is also important. First, it will be significant to know under what conditions they behave differently from diblocks. This will help define the applicability of the extensive diblock copolymer literature to particular applications. Also, it is reasonable to expect that graft copolymers and other more complex copolymer structures will exhibit quite different behavior that will have relevance to applications.

Our graft copolymers consisted of poly(ethyl acrylate) (PEA) backbones onto which polystyrene (PS) grafts were attached at random sites. They are called

*Current address: Dept. of Physics, Illinois Wesleyan University, Bloomington, IL 61702

"model" materials because their structures are expected to be somewhat better-defined than *in situ* compatibilizers. Preliminary results are presented here from small-angle neutron scattering (SNS), neutron reflection (NR), and transmission electron microscopy (TEM).

EXPERIMENTAL

Synthesis

The PEA-g-PS materials were synthesized by a macromonomer technique [5]. Monodisperse PS chains, having a total numbered-averaged molecular weight (M_n) of 14.6 kg/mol and a methacrylate endgroup, were added to partially deuterated ethyl acrylate monomer [6] and polymerized via free radical polymerization. The PS chains then were included at random as grafts onto the PEA backbone. Each of the resulting graft copolymer materials had a (M_n) of $\approx$ 150 kg/mol. Three compositions were prepared, having 9, 28, and 48 wt% PS grafts, corresponding to an average of 1, 3, and 5 PS grafts per molecule, respectively.

Small-Angle Neutron Scattering

Thick ($\approx$ 0.5 mm thickness) films were prepared for SANS by melt pressing. The samples were annealed in the press for 6 hours at 130°C. Squares (2.5 cm $\times$ 2.5 cm) were cut from the films in a stretching device that allowed for the application of a uniaxial strain. The stretching device could then reach a maximum elongation ratio $\lambda(\lambda = \Delta l/l_0)$ of about 3. We applied strain to the samples in steps, never allowing it to relax until the measurements were complete, a time period on the order of one day. Of course, because the PEA component is elastomeric, there would be some relaxation of stress in the material. Upon releasing the clamps after the measurements were completed, the samples would typically not return very much toward their original length. We were able to stretch the 9 wt% material to the limit of the device, but the 28 wt% would usually break before reaching $\lambda = 2$, and the 48 wt% PS material could not be stretched in this manner at all. SANS measurements were performed on the NG7 instrument at the National Institute of Standards and Technology and SAD at Argonne's Intense Pulsed Neutron Source (IPNS).

Neutron Reflection

We prepared thin (1000–2000 Å thickness) film samples for NR study by spin-coating from toluene solution onto silicon substrates. The substrates were prepared beforehand by soaking in chromic sulfuric acid, rinsing in deionized water, and rinsing with toluene. The film thicknesses were determined by ellipsometry. The samples were then annealed in a vacuum over ($\approx$ mT) for 24 hours at 130°C.

Neutron reflection data were obtained on POSY-II at IPNS [7]. NR is an effective means to determine the chemical depth profile in systems that have been labeled for neutron contrast. The details of the NR technique have been considered elsewhere [8]. The reflectivity $R(k)$, where k is the momentum transfer vector

normal to the sample plane,

$$k = \frac{2\pi}{\lambda} \sin \theta, \tag{1}$$

(where θ is the angle of incidence/reflection) is a phaseless, non-linear transform of the depth profile. No inverse transform has been developed, so the typical procedure is to fit the parameters of a model profile to the data via χ^2 minimization.

Transmission Electron Microscopy

Thin sections of the samples for analysis with transmission electron microscopy were prepared by first staining the as-cast film (prepared as explained above for the SANS samples) with RuO_4 vapors, then shaping the cutting surface and then making final cuts with a cry-microtome held at approximately $-90°C$. The resulting thin sections were mildy stained a second time with RuO_4 vapors before analysis to enhance the contrast. Bright field images were obtained using a Philips EM420ST transmission electron microscope operated with an accelerating voltage of 100 kV.

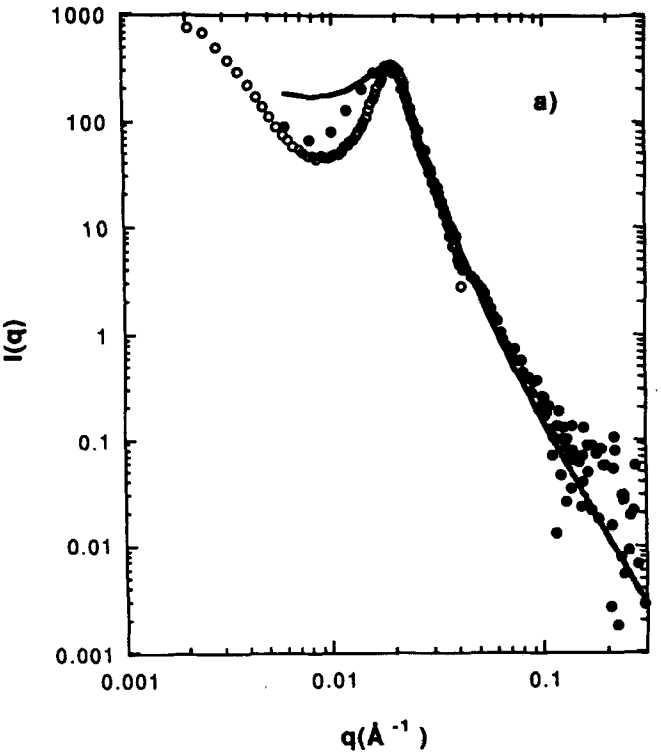

FIGURE 1 Small-angle neutron scattering spectra from each of the three materials studied. a) 9 wt% polystyrene grafts, b) 28 wt% PS grafts and c) 48 wt% PS grafts. The open symbols are National Institute of Standards and Technology data and the solid symbols are Argonne's Intense Pulsed Neutron Source data. The solid lines are fits to Equation (2).

RESULTS AND DISCUSSION

Small Angle Neutron Scattering

Unstretched samples: The SANS spectra from each of the three samples are shown in Figure 1. In these data sets, the two-dimensional data were integrated around the full circle. There is a single scattering peak in each spectrum. In order to characterize this peak, we fit the data with the following expression:

$$S(q) \propto \frac{1/q^{\alpha}}{1 + (q - q_0)^2 \xi^2}, \tag{2}$$

where q is the scattering vector, given by:

$$q = \left(\frac{4\pi}{\lambda}\right)\sin\left(\frac{\theta}{2}\right), \tag{3}$$

where λ is the neutron wavelength and θ is the scattering angle.

This functional form was chosen because it fit the data well (at medium to high q) and allowed us to characterize the width (via the "correlation length ξ) and position (via q_0) of the scattering peaks and the exponent describing the high q

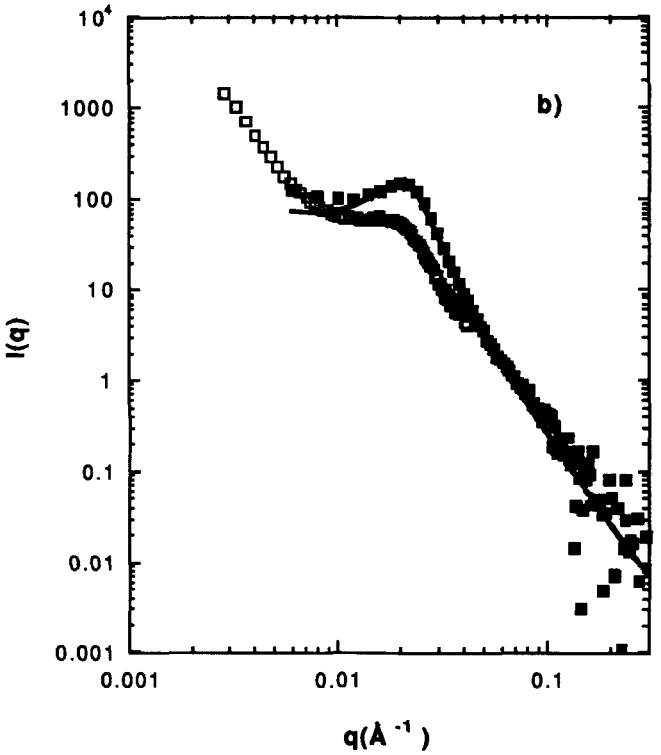

FIGURE 1 (*Continued*)

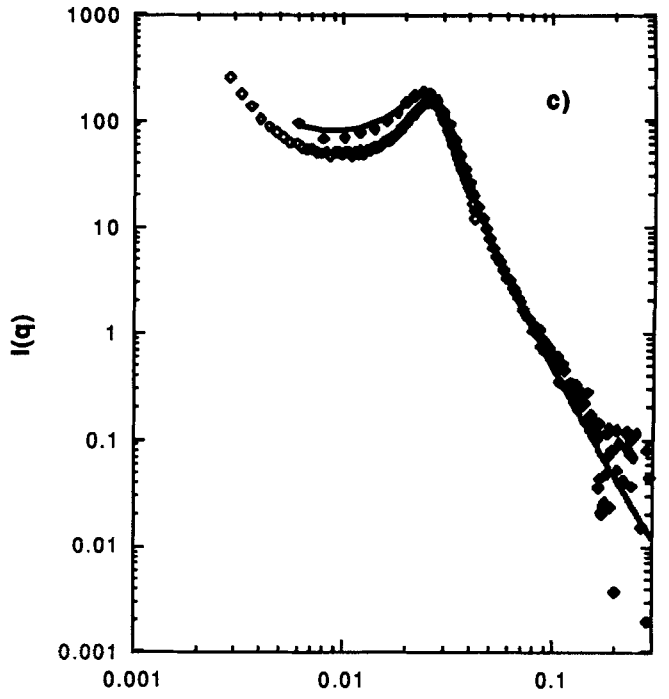

FIGURE 1 *(Continued)*

decay (given by $\alpha + 2$). From the position of the peak, we can determine an average domain spacing, L. The correlation length is a measure of the strength of the ordering in the sample. The resulting parameters are shown in Table I. As would be expected, the spacing between PS domains decreases as the grafting level increases (i.e., L decreases as the volume fraction of PS increases). The "correlation length," ξ, is quite short—shorter than the domain spacing—indicating that the order in these bulk samples is rather weak.

It is difficult to accurately determine the high q exponent with SANS, because of the incoherent scattering background due to the protons in the samples. In fitting the data, the resulting exponents turn out to be slightly larger than 3, which would indicate rough interfaces between the domains. This parameter, however, was fairly soft in the fits due to the incoherent scattering (hence the resulting values are not shown here), and SAXS experiments are planned to quantify the interfacial structure.

TABLE I. Results from SANS f_{PS} is the weight fraction of PS grafts, the other quantities are as defined in Equation (2).

f_{PS}	q_0, Å^{-1}	$L \approx \frac{2\pi}{q_0}$, Å	ξ, Å
0.09	0.0190	330	200
0.28	0.0213	295	155
0.48	0.0255	245	140

The data do not agree with Equation (2) at small q; in fact, the data appear to turn up at small q. This is indicative of some additional correlated contrast at longer length scales. This is possibly due to the phase separation of ungrafted PEA homopolymer, which will be discussed further below.

Note that in Figure 1 and all later figures containing SANS data, we have subtracted an estimated constant background for each sample due to incoherent scattering from protons (determined from the highest-q region, typically $q > 0.2$ Å^{-1}, where the raw data are practically constant). Also note that the SANS curves

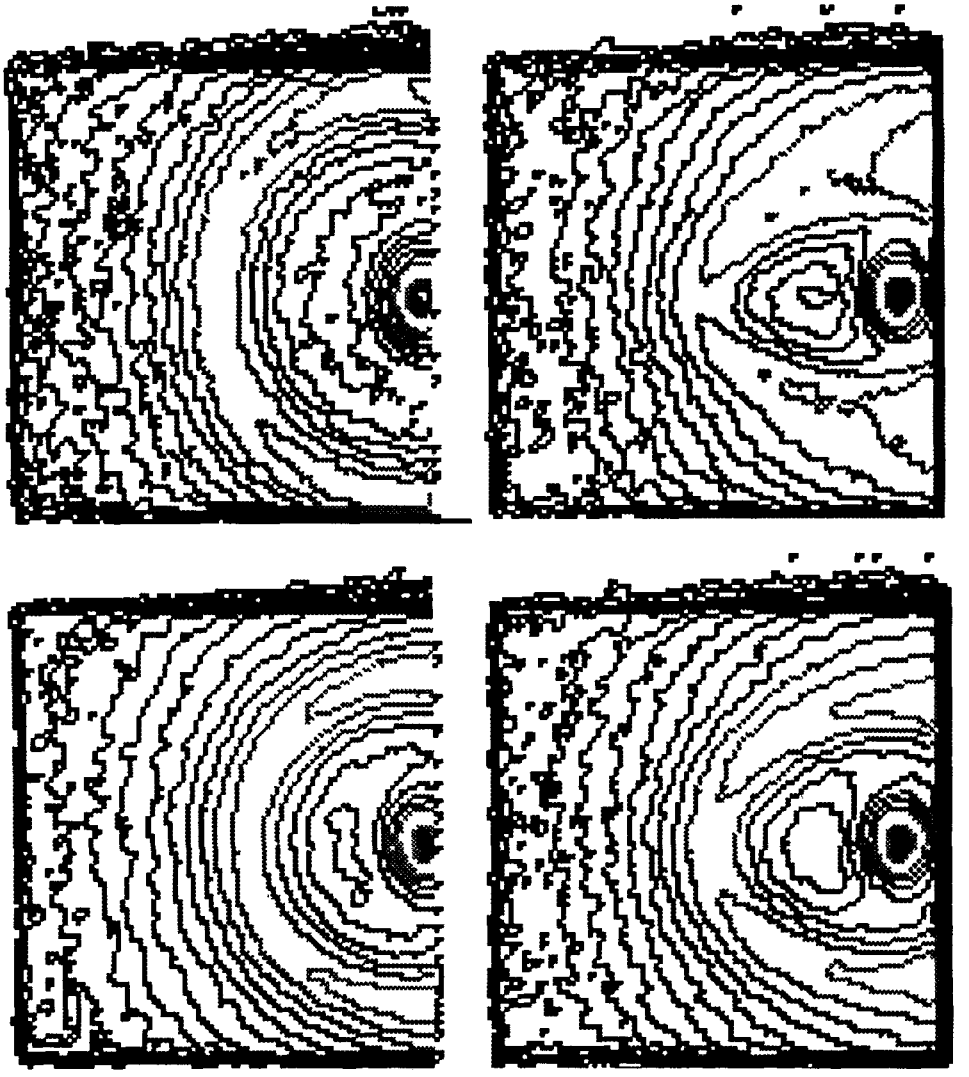

FIGURE 2 Two-dimensional contour plots of Small-angle neutron scattering spectra from 9 wt% sample undergoing uniaxial strain. The stretching direction is vertical in all plots, with the range of q in each the same as that of the National Institute of Standards and Technology data in Figure 1. The elongation ratios are, counter-clockwise from top left, 1.00, 1.50, 2.00, 3.00. The highest q shown in these figures is ≈ 0.02 Å^{-1}.

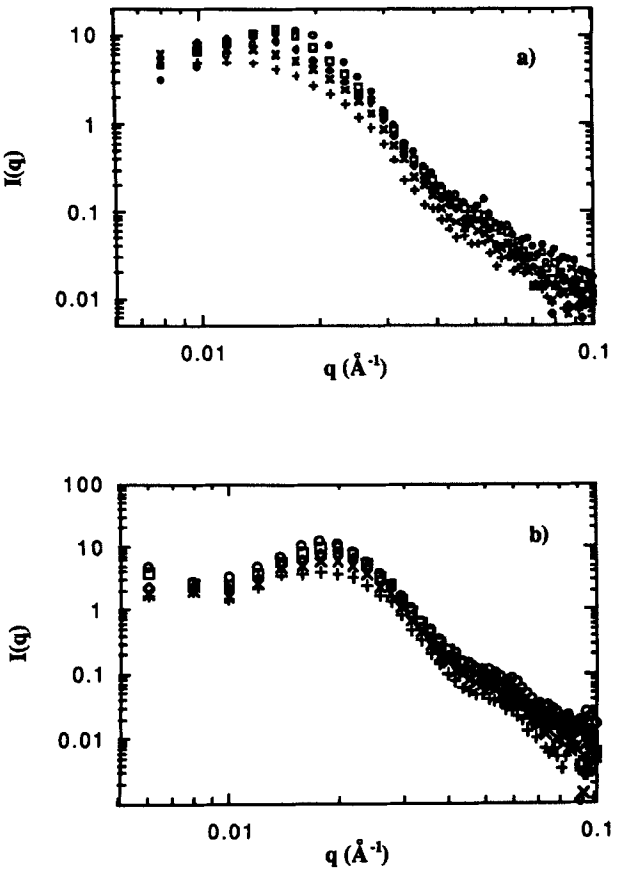

FIGURE 3 Wedge-averaged intensity data from 9 wt% polystyrene sample, in directions a) parallel to, and b) perpendicular to the stretching direction. The circles, squares, diamonds, x's and crosses correspond to elongation ratios of 1.00, 1.20, 1.50, 2.00 and 3.00, respectively.

are normalized as well as possible on an absolute scale, and that the data from the two instruments agree reasonably well. The apparent differences between the data sets in their overlap regions are due the differences in resolution of the two instruments and small differences in the samples measured (the thicknesses were reproducible only within 5–10%, for instance).

Stretched samples: The two-dimensional SANS spectra for the stretched 9 wt% sample are shown in Figure 2. The pattern in Figure 2 is the usual "two-point" elliptical one seen in strained rubbers. Rather than integrating the full circle as is typically done in SANS, we integrated the data in wedges that were $\pm 30°$ from either the stretching direction or the direction perpendicular to it. This particular wedge was determined to be the widest wedge that would not excessively smear the data. The resulting curves are shown in Figure 3. These curves can in turn be fitted by Equation (2), and the resulting positions and widths of the scattering peaks as a function of the elongation ratio for the 9 wt% PS sample are shown in Figure 4.

The position of the peak in the stretching direction is a linear function of the elongation ratio λ, whereas that in the perpendicular direction appears to be

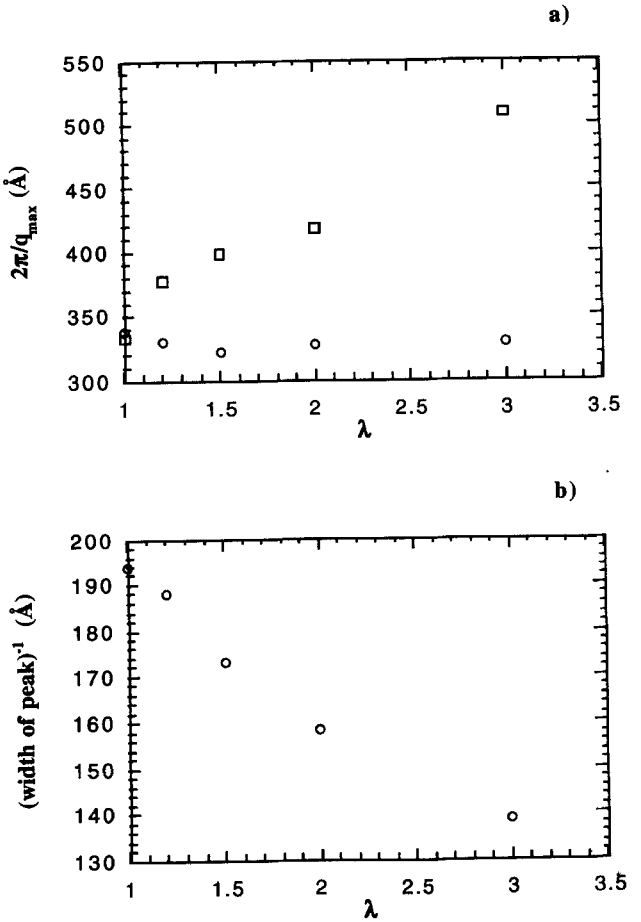

FIGURE 4 The a) position and b) width of the scattering peaks in the data from Figure 3 (circles: parallel to stretch, squares, perpendicular to stretch), as a function of the elongation ratio.

independent of λ. This is characteristic of a quasi-affinedeformation. In as much as one would expect that the morphology of this sample is some quasi-periodic arrangement of PS spheres or cylinders in a d-PEA matrix, this behavior is not surprising.

Two-dimensional contour plots of the SANS from a 28 wt% PS sample are shown in Figure 5. Note the appearance of lobes in the scattering pattern that grow parallel to the stretching direction. These "abnormal butterfly" patterns [9–12] appear even at low values of λ. We have observed similar patterns in these samples via light scattering, indicating that its origin is at long ($\gtrsim 1$ μm) length scales. Looking at the higher-q regions of the contour plots and at the IPNS data (which does not include much of the butterfly-like data in the low-q region below the peak), we can see the scattering pattern change over to one that is more like the conventional elliptical pattern [13]. In fact, applying a function like Equation (2) to wedge-integrated data (higher-q) data (shown in Figure 6) results in anisotropy in L, but not in ξ (see Figure 7). In butterfly patterns arising from gels, the "correlation length" is typically quite anisotropic [12]. In Figure 7a we again

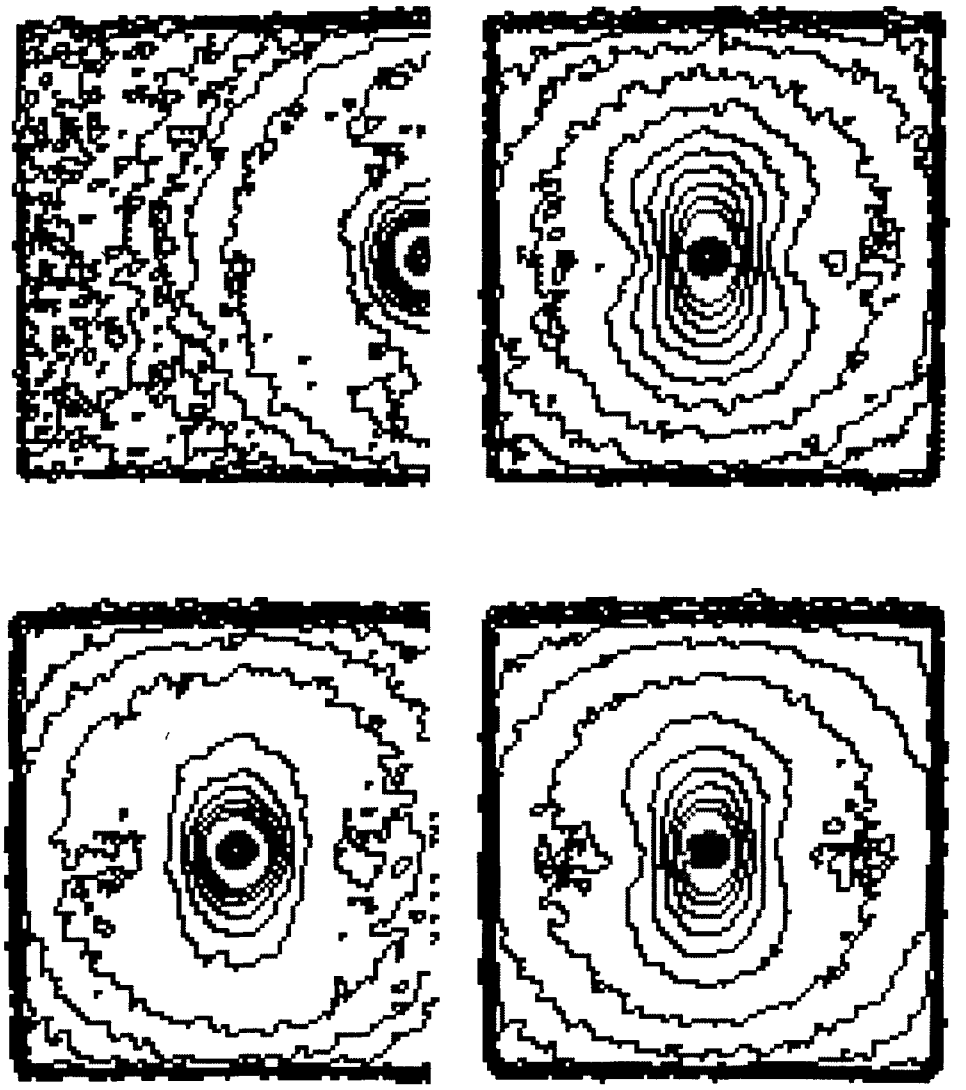

FIGURE 5 Two-dimensional contour plots of Small-angle neutron scattering spectra from 28 wt% sample undergoing uniaxial strain. The stretching direction is vertical in all plots, and the range of q in each is the same as that of the National Institute of Standards and Technology data in Figure 1. The elongation ratios are, counter-clockwise from top left, 1.00, 1.08, 1.28, 2.35. As in Figure 2, the highest q shown here is ≈ 0.02 Å^{-1}.

see that the spatial period in the direction parallel to the strain increases (but probably not in a linear fashion for this sample) as the sample is stretched and that the periodicity in the perpendicular direction changes very little.

Neutron Reflection

Specular neutron reflectivities are plotted for the three materials in Figure 8, along with the fitted curves (solid lines) produced using model depth profiles of the

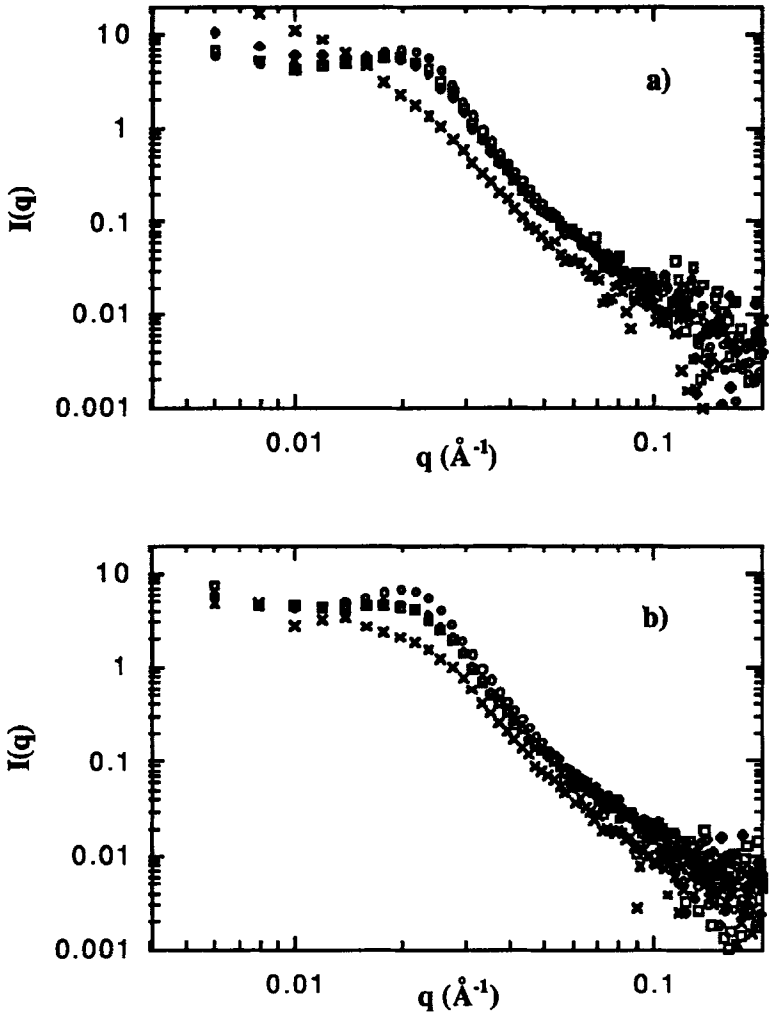

FIGURE 6 Wedge-averaged intensity data from 28 wt% polystyrene sample, in directions a) parallel to, and b) perpendicular to the stretching direction. The circles, squares, diamonds and x's correspond to elongation ratios (λ) of 1.00, 1.08, 1.28 and 2.35, respectively.

following form [14,15]:

$$\phi(z) = \phi_0 + (e^{-z/\delta} + e^{(z-z_0)/\delta}) \sum_i \left[a_i \cos\left(\frac{2\pi z}{L}\right) + b_i \sin\left(\frac{2\pi z}{L}\right)\right], \tag{4}$$

where $\phi(z)$ is the volume fraction of PS (the minority component) as a function of depth, L is the spatial period of the structure, z is the distance from the substrate surface, z_0 is the total film thickness, ϕ_0 is the average volume fraction of the minority component, δ is the characteristic distance over which the ordering (or orientation) persists away from the interfaces and a_i and b_i are free parameters. We used

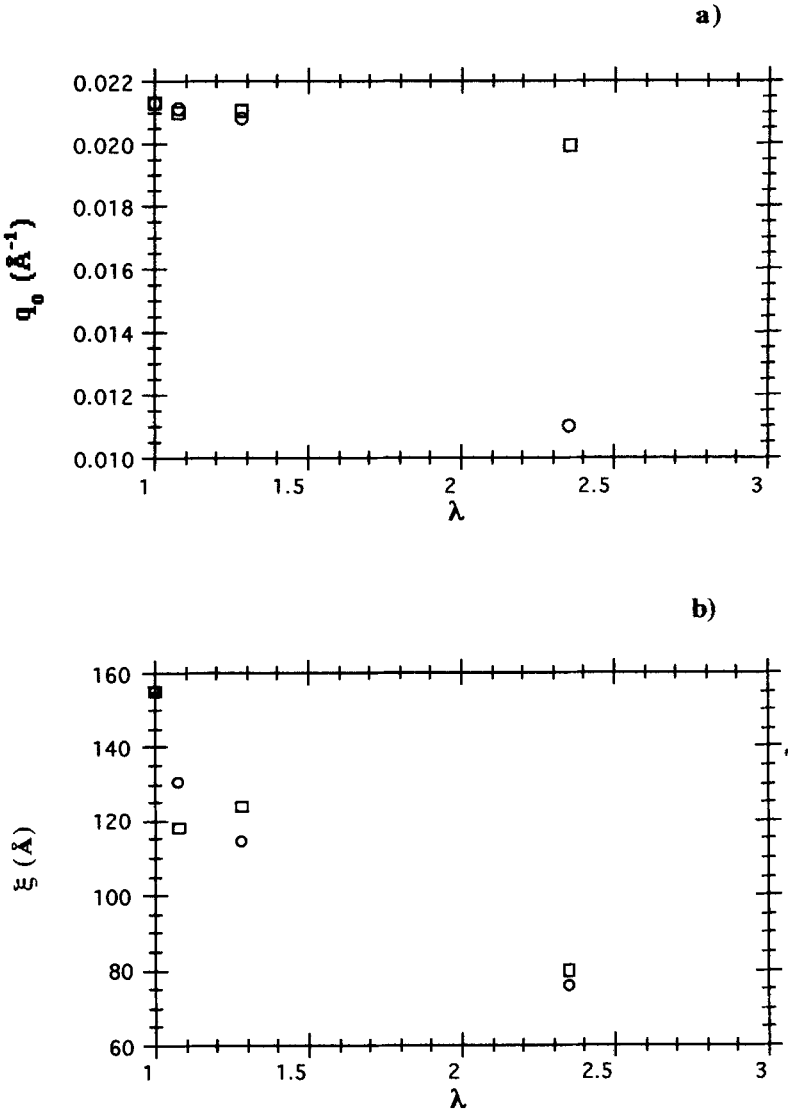

FIGURE 7 The a) position and b) width of the scattering peaks in the data from Figure 6 (circles: parallel to stretch, squares, perpendicular to stretch) as a function of the elongation ratio.

1.43×10^{-6} Å^{-2} for the scattering length density of PS and measured the scattering length density for the partially deuterated PEA to be 4.38×10^{-6} Å^{-2}. This model assumes that the orientation or ordering is induced and/or pinned at the interfaces and that the spatial period is constant throughout the sample. As the available window in q-space is limited, we can only use $i \leq 3 - 4$ in the fits. Model-free treatment of the data via a maximum entropy technique [16] produced similar profiles. Some of the important parameters from Equation (4) used to fit the NR data are listed in Table II. It should be noted that this model profile is not necessarily the best one to use; lower-resolution, direct space techniques like

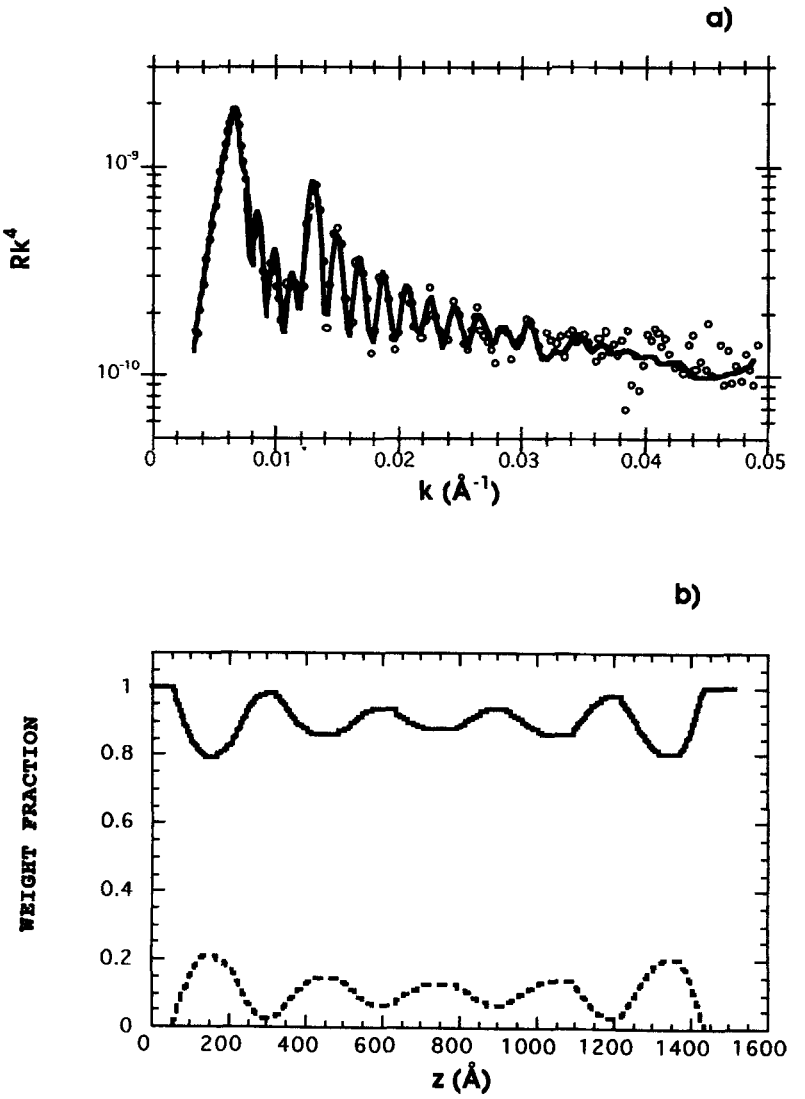

FIGURE 8 Specular neutron reflectivities and fitted real-space profiles for each of the three materials, annealed 24 h at 130°C: a) & b) wt% polystyrene, c) & d) 28 wt% polystyrene and e) & f) 48 wt% PS. In profiles, solid lines are PEA and dashed lines are PS.

secondary ion mass spectrometry (SIMS) will be used in the future and may lead to a better choice of model.

The NR-fitted profile from the 9 wt% PS sample shows a periodic structure that propagates through the film. This profile would fit well with an hypothesis that this sample has a morphology consisting of an ordered array of spheres or cylinders. The 48 wt% PS film, however, shows only evidence of surface-induced orientation.

The NR data from the 28 wt% PS thin films can only be successfully modeled with a lamellar profile, with alternating layers of 100% PEA and nearly 100% PS. This is a surprising result. Given the architecture of the graft copolymers, one

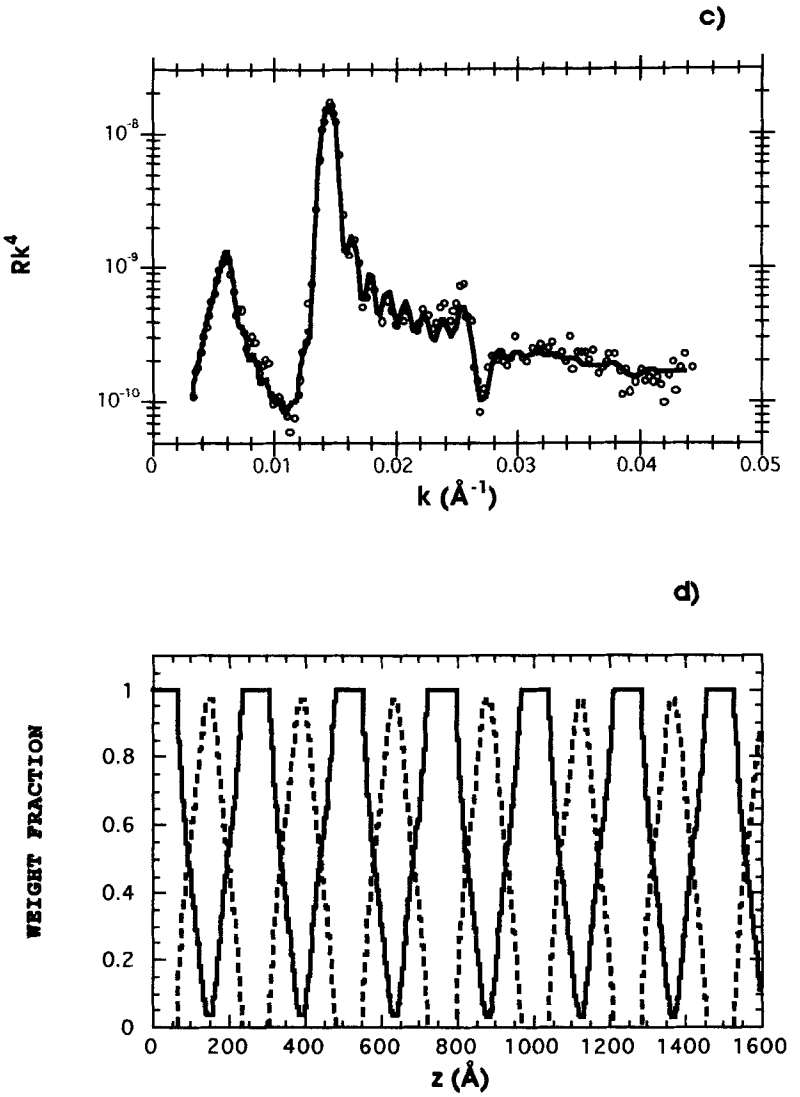

FIGURE 8 (*Continued*)

expects the PEA-PS interface to bend strongly toward the (PS) graft component, even for compositions > 50% PS. In fact, one can estimate what composition will give rise to a flat interface by using a modified form of a criterion for flat interfaces in diblock copolymer melts [17]:

$$\phi_{PS}^2 a_{PS} \sigma_{PS}^3 = \phi_{PEA}^2 a_{PEA} \sigma_{PEA}^3 . \tag{5}$$

where σ is the areal density of chains, ϕ is the volume fraction of a given species and a is the "packing length," a measure of the flexibility of the chain (given by: $a = 3m_0/C_\infty b^2 \rho$, where m_0 is the mass per backbone bond, ρ is the polymer density, b is the bond length and C_∞ is the characteristic ratio). For diblocks,

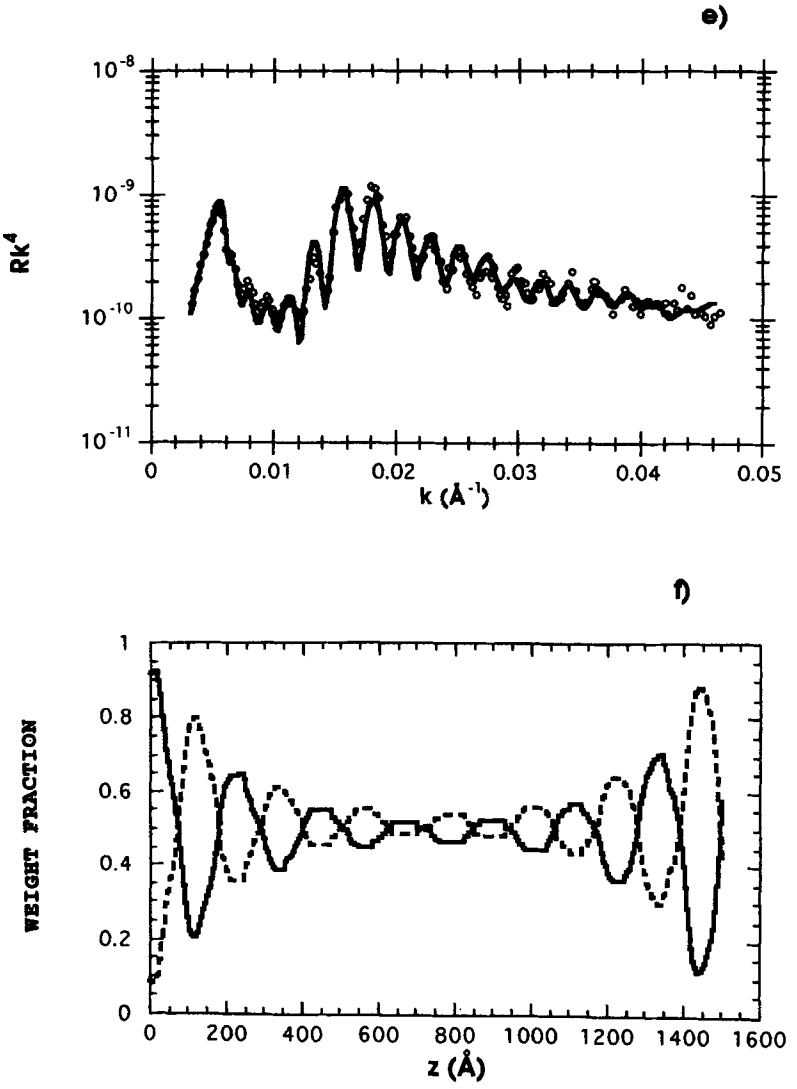

FIGURE 8 (*Continued*)

TABLE II. Results from NR, f_{PS} is the weight fraction of PS grafts, the other parameters are as defined in Equation (4).

f_{PS}	L, Å	δ, Å
0.09	293	295
0.28	244	∞
0.48	220	180

$\sigma_A = \sigma_B = \sigma$, but for graft copolymers there are two backbone chains for each graft chain at the interface, so $\sigma_{PEA} = 2\sigma_{PS} = 2\sigma$. Inserting literature values for the a's leads to the conclusion that a flat interface will result with a composition of 72% PS.

Transmission Electron Microscopy

Figure 9 is a transmission electron micrograph of a 28 wt% PS sample (the dark areas are the PS). Note the "fingerprint"-like appearance that is characteristic of lamellae microstructures. Note also that there are a few dots in the picture that could possibly be cylinders viewed end-on. However, with the degree of orientational disorder present in this sample, any random view through overlapping arrays of cylinders would produce a range of Moiré patterns. This does not occur, so we either do not have cylinders or the view shown in Figure 9 is a carefully chosen orientation of a highly aligned sample. The latter is not probable given the lack of orientational order present. The lamellae do seem, however, to bend over a length that is only a few times the spatial period. This is in qualitative agreement with the SANS data that shows relatively weak ordering in the bulk samples. The structure of bulk samples of the 28 wt% PS material could well be that of "tortuous lamellae," meaning lamellae with irregularly modulated interfaces. The staining contrast shows a modulation in the PS layers which we conjecture is due to local variations in graft density. Regions that show isolated "dots" may be due to lamellae that are nearly parallel to the page so that the strongly stained regions give dot patterns. Further investigations will be required to fully define this morphology.

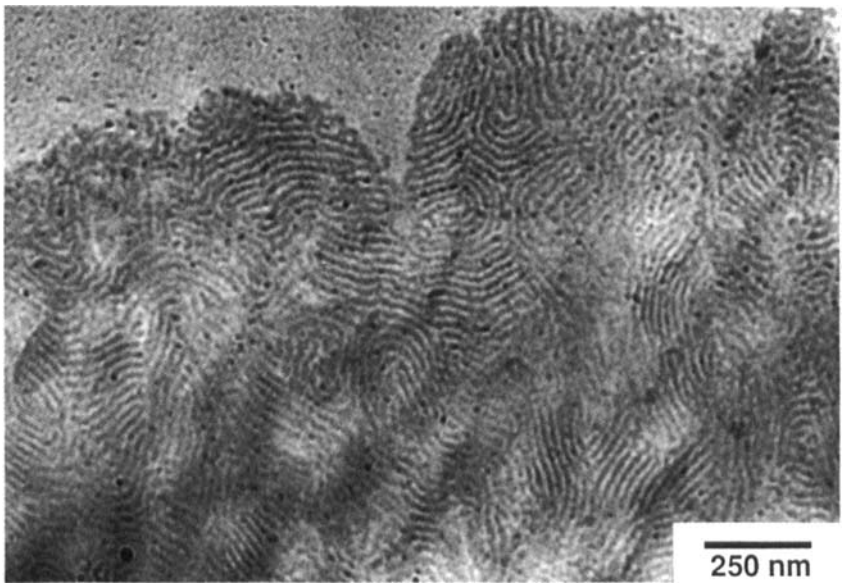

FIGURE 9 Transmission electron micrograph of 28 wt% polystyrene sample stained with ruthenium tetroxide.

We have two principal hypotheses as to the origin of this lamellar phase. First, it is well established that polydispersity will reduce the elastic energy in a polymer melt [18]. Therefore, we expect that the polydispersity of the backbone molecular weight will lead to less than expected elastic energy and hence less than expected curvature of the interface towards the graft component. This effect is in the right direction, but its magnitude is unknown in this case.

The other, and probably more important, possible cause for this result is the randomness of the graft placements. There are, no doubt, may attachments where the molecular weight between grafts is very small. This situation will lead to more phase mixing on the PS side of the PS-PEA interface. This is probably what is seen in modeling the NR data. Note that the model profile has layers of 100% PEA, but that the PS layers never quite reach the pure PS level. Note also that the alternating layers are nearly equal in thickness. This appears to be the case in the TEM photo as well. If it were not so this would be reflected in the second order Bragg peaks in Equation (4) and therefore easily visible in the NR data. All of these characteristics are consistent with the randomness of graft placement causing phase mixing at the interface.

CONCLUSIONS

We have characterized a family of PEA-g-PS model graft copolymer compatibilizers via SANS and NR. In doing so, we have found that these copolymers are strongly phase separated into quasiperiodic structures. The bulk samples exhibited rather weak ordering, whereas ordering appeared to be enhanced (at least in two of the three samples) by the interfaces present in thin film samples. One of these materials produced abnormal butterfly patterns in SANS spectra and a lamellar morphology in spite of its highly asymmetric composition and random architecture. Further work is planned and/or underway on these materials: SAXS, to determine the high-q (Porod) exponent that will give some additional information as to the structure of the PEA-PS interface in the neat copolymer, SANS on homopolymer blends to test directly the compatibilization as a function of grafting level and SIMS on thin films to uniquely determine the shape of the density profile.

Acknowledgments

The technical assistance of P. Wright, M. Olveria, R. Goyette, and D. Wozniak and helpful discussions with M. Olvera de la Cruz, T. Witten, A. Karim, and N. Singh are gratefully acknowledged. The neutron reflection data was collected with the assistance of G. Agrawal. Work at Argonne is supported by US DOE, BES-MS contract #W-31-109-ENG-38.

References

1. F. S. Bates, *Science*, **251**, 898 (1991).
2. L. A. Utracki, D. J. Walsh and R. A. Weiss, *Polymer Alloys, Blends and Ionomers*, American Chemical Society: Washington, D.C., 1989.
3. M. Lambla and M. Seadan, *Polym. Eng. Sci.*, **32**, 1687 (1992)

4. M. Xanthos and S. S. Dagli, *Polym. Eng. Sci.*, **31**, 929 (1991)
5. M. Rabeony, D. G. Peiffer, W. D. Dozier and M. Y. Lin, *Macromolecules*, **26**, 3676 (1993).
6. W. D. Dozier, D. G. Peiffer, M. Y. Lin, M. Rabeony, P. Thiyagarajan, G. Agrawal and R. P. Wool, *Polymer*, **35**, 3116 (1994).
7. A. Karim, B. H. Arendt, R. Goyette, Y. Y. Huang, R. Kleb and G. P. Felcher, *Phys. B*, **173**, 17 (1991).
8. T. P. Russell, *Mat. Sci. Rep.*, **5**, 171 (1990).
9. R. Öser, C. Picot and J. Herz, *Spring. Proc. Phys.*, **29**, 104 (1987).
10. R. Öser, Ph. D. Thesis, Johannes Gutenberg Universität, Mainz, 1992.
11. J. Bastide, F. Boué and M. Buzier, *Spring. Proc. Phys.*, **29**, 112 (1987).
12. J. Bastide, L. Leibler and J. Prost, *Macromolecules*, **23**, 1821 (1990).
13. F. Boué, J. Bastide, M. Buzier, A. Lapp, J. Herz and T. A. Vilgis, *Colloid Polym. Sci.*, **269**, 195 (1991).
14. N. Singh, M. Tirrell and F. S. Bates, *J. Appl. Crystallogr.*, **26**, 650 (1993).
15. M. D. Foster, M. Sikka, N. Singh, F. S. Bates, S. K. Satija and C. F. Majkrazk, *J. Chem. Phys.*, **96**, 8605 (1992).
16. D. S. Sivia, W. A. Hamilton and G. S. Smith, *Phys. B*, **173**, 121 (1991).
17. T. A. Witten, S. T. Milner and Z.-G. Wang, in *Multiphase Macromolecular Systems*, B. M. Culbertson, Ed., Plenum: New York, 1989.
18. W. W. Graessley, *Adv. Polym. Sci.*, **16**, 1 (1974).